The Living Light Conference 2016

Investigation of the Variation of Near-Circular Polarization in Scarabaeoidea Beetles[*]

IE Carter[*], K Weir and MW McCall

Blackett Laboratory, Department of Physics, Imperial College London, London, SW7 2BZ, UK

Abstract

Variation in the reflection of circularly polarized light (CP) of a substantial number of beetles, of both the Hybosoridae and Scarabaeidae families, is discussed. Classifications of the spectral shapes were made for *Cetonia aurata aurata* beetles, which were related to variations within the chiral chitin structure and have been computationally modelled. It was seen that single peaked spectra were not the predominant spectral shape and that more complex structures are responsible for the spectra observed. Two structural perturbations methods to the single pitched structure are proposed to be responsible for the more complex spectral shapes. Further CP analysis of the genus rutelinae:*Chrysina* was undertaken with variations in broadband reflection observed within the *optima* species.

Keywords: circular polarization; scarab beetles; chiral; structural helicity; birefringent; chitin;

1. Introduction

Circularly polarized (CP) light is relatively uncommon in nature. One of the first described examples was a golden beetle (*Chrysina resplendens*), which Michelson described as having a "screw-like structure" [1]. From the plant world the fruit of the genus *Pollia,* which is a metallic blue, reflects both left CP (LCP) and right CP (RCP) light [2]. It has also been observed that LCP light leads to faster growth in pea and lentil plants [3]. From the animal

_____

world the mantis shrimp (*Odontodactylus*), is able to visually detect and also signal with reflections of CP light [4][5]. Another group which interacts with CP light is *Sapphirinidae* Copepods, where light passing through their bodies becomes CP [6]. There are several species of firefly (*Photuris lucicrescens* and *Photuris versicolor*) whose larvae are CP bioluminescent, and emit LCP and RCP light from opposite lanterns [7]. In the non-living world arrangements such as a water-air interface can produce CP light via total internal reflection [8], as well as in light emitted by some stars [9].

Since Michelson's first observation of such a reflection, there has been interest in CP reflections from scarabs from many difference disciplines [10]. Preliminary work by Pye showed the CP reflection distribution in nine different subfamilies (Fig. 1) [11]. Fossil records of structural color in beetles stretch back 15-47 million years [12].

The origin of the CP reflection is within the beetle's shell (epi- exocuticle layers). It is formed of layers of chitin, which are thread-like molecules, embedded in a protein matrix, all of which have the same orientation. Between adjacent layers the direction of the molecules in the layer gradually alters. As the layers build up eventually a pitch (full 360° rotation) in the orientation of the molecules is achieved [13]. The thread-like nature of the molecules means there is a birefringence in the material, which is enhanced by the presence of uric acid [14]. The pitch (p) of the structure is related to the reflection peak observed at wavelength (λ_p),

$$\lambda_p = \overline{n}(\lambda)\,p \qquad\qquad (1)$$

where $\overline{n}(\lambda)$ is the average refractive index of chitin [15].

Most previous studies on CP reflection in beetles have focused on few specimens, often single examples of a species [15,16]. In this study a near-normal CP reflection from a large number of beetles mainly of Cetoniinae and Rutelinae, but also of the Ceratocanthinae, Scarabaeinae, Trichiinae, Phaenomeridinae, Dynastinae, Melolonthinae and Euchirinae subfamilies are studied. In this way the variation, or 'finger-print', of spectra of several species and genus can be quantified. While a number of beetles in each group have been examined, in this report typical examples of each of the subfamilies are presented, followed by a study of variation amongst 191 *Cetonia aurata aurata* beetles, and a study of color variation amongst *Chrysina optima*.
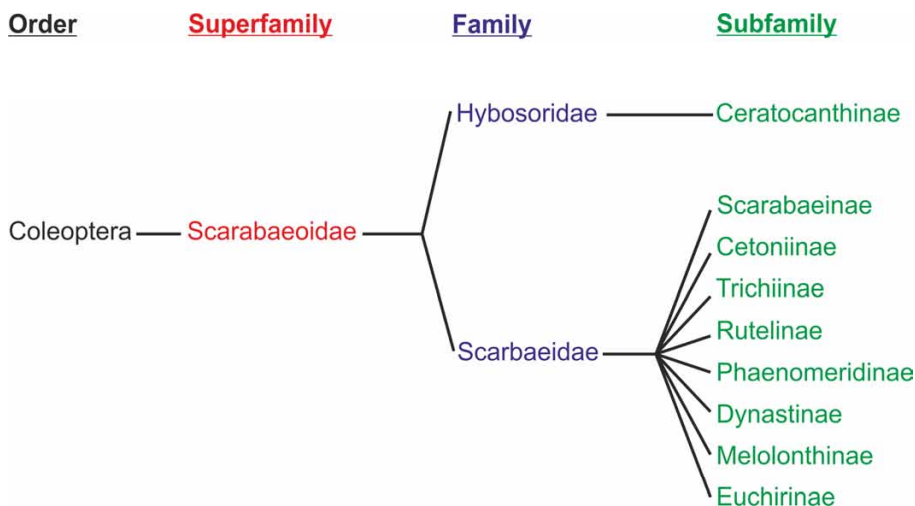

Fig. 1. Taxonomic map of subfamilies that contain optically active Coleoptera.

2. Method and Specimens

2.1. Specimens

Specimens from all 9 subfamilies seen in Fig. 1 were investigated. The collection location of each specimen can be seen on the world map in Fig. 2. The length of the beetles from the bottom of their elytra to the top of their pronotum varied from 2 mm (Ceratocanthinae:*Ceratocanthus sp*.) to 52 mm (Euchirinae: *Cheirotonus battareli*).

Fig. 2. Collection locations of specimens: 1. Ceratocanthinae:*Ceratocanthus sp*. 2. Scarabaeinae:*Diabroctis mimas.* 3. Cetoniinae:*Protaetia angustata pyrodera.* 4. Trichiinae:*Gnorimus nobilis.* 5. Rutelinae:*Viridimicus aurescens.*6. Phaenomeridinae:*Phaenomeris besckei.* 7. Dynastinae:*Augoderia nitidula.* 8. Melolonthinae:*Melolontha melolontha*. 9. Euchirinae: *Cheirotonus battareli*. Map made from [18].

Specimens of the Rutelinae:*Chrysina* genus were also investigated which were all collected in Costa Rica. The specimens varied from 23-30 mm in length. Cetoniinae:*Cetonia aurata aurata* specimens were also investigated, which were collected from various sites throughout Romania and Poland. The specimens measured between 14 and 21 mm in length.

2.2. Reflection Spectroscopy Experimental Setup

The measurements were taken using the system shown schematically in Fig. 3. A halogen light source (DH2000-BAL) (430-1000nm) [19] was coupled into an optical fiber (QP600-2-SR-BX), the beam was then collimated and polarized to become CP light. The CP light was produced by first passing unpolarised light through a polarizing cube, which was set to give either ±45° linearly polarized light with respect to the axis of the Fresnel rhomb. In the Fresnel rhomb two internal reflections occur, which produces a $\pi/2$ phase shift, converting the linearly polarized light into CP light [20]. The handedness of the CP light (LCP or RCP) is determined by angle of polarization of the input linear light.
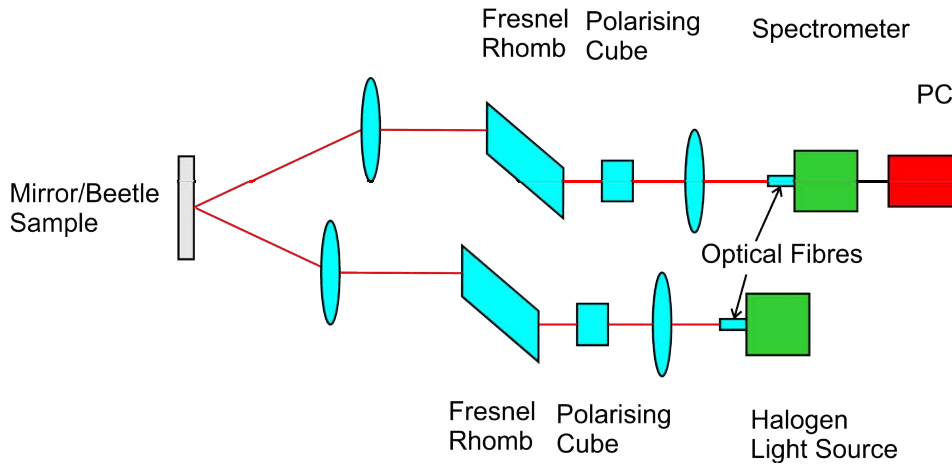
Fig. 3. Reflection spectroscopy experimental setup.

The light spot size is ~1mm in diameter and was usually focused on the top of the beetle's right elytra. The reflected beam was then collected with a lens and the CP light was passed through the Fresnel rhomb followed by the polarizing cube in a similar arrangement to the input stage. The input and collecting arms are at 45° (22.5° incident angle) to each other to allow space for the optical components. The orientation of the polarizing cubes could be changed between ±45° to analyze LCP and RCP light. The spectrum was measured using an Ocean Optics HR4000 spectrometer. Further details of the experimental setup can be found in [21]. A reference was obtained using a flat front-silvered mirror with the reflectance from the beetle calculated as

$$Reflectance = \frac{Signal(beetle) - Background}{Reference(mirror) - Background},\qquad(2)$$

where Signal(beetle) is the signal of the light reflected from the beetle and Background is the dark response. In the study four CP combinations were made:

- LL   - LCP light incident, LCP analyzed,   LR   -   LCP light incident, RCP analyzed,
- RL   - RCP light incident, LCP analyzed,   RR   -   RCP light incident, RCP analyzed.

2.3. Modelling

The modelling was used to compare to the experimental spectra data. The model was implemented as a multilayered transfer matrix method using the Birefringent Film Toolbox described in [22]. The model had perturbations to the single pitch structure (which results in a single spectral peak). The perturbations to the spectra were based on 2 structural changes to the model. The first perturbation was several different pitch thicknesses being present, resulting in several peaks in the reflection spectra (Fig. 4a) [16] . The second perturbation is a sudden jump in the orientation angle of the chitin molecules between adjacent layers (Fig. 4b) [23].

The models do not consider any structures within the beetle responsible for the spectra other than a helicoidal structure. The first spectrum (Fig. 5(a)) was created using two different pitch values, the second (Fig. 5(b)) was modelled using the sudden jump in orientation of the molecules. The parameters used in all of the models within this paper are summarised in the Appendix.
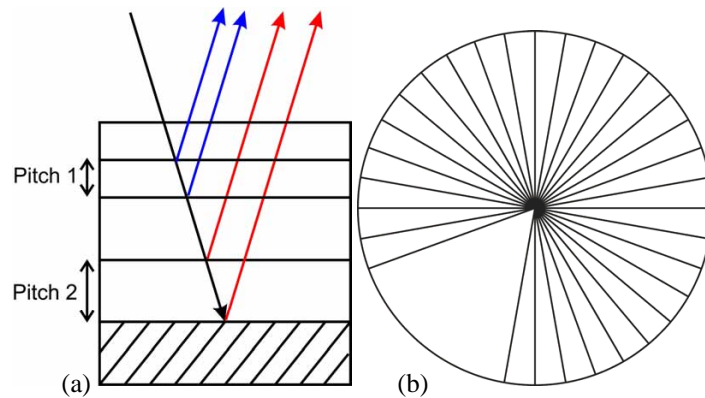
Fig. 4. Structural perturbations of the helicoidal chitin within the beetle's shell of (a) multiple pitches (side view) (b) sudden jump in the orientation of the chitin molecules (top view).
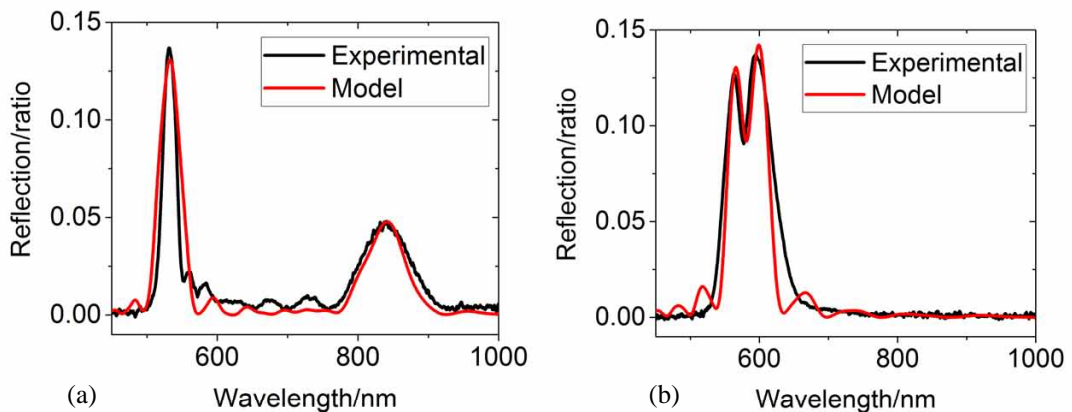

Fig. 5. Experimental and modelling CP reflection spectra compared, for Cetoniinae:*Lomaptera* (a) *geelvinkiana (*using birefringent refractive indices of 1.485+0.01i and 1.52+0.01i, having a thickness of 12.5 pitches in total) and (b) *pygmeae* (modelled with a discontinuity in the pitch of 8/15 π, using complex birefringent refractive indices, of 1.46+0.025i and 1.52+0.025i , and a layer 11 pitches thick in total). Further details of the model and parameters are given in reference [21].

3. Results

3.1. Reflectance Spectrometry

The results are presented in the context of three separate but related studies; a broad suvey of the families, a statistical study of the variation across 191 *Cetonia aurata aurata* and an initial examination of the variation within and between species of *Chrysina*.

Reflection spectra were obtained with the four CP combinations and the LCP response modelled as above. In the following figures the experimental data is presented with the modelled LL response superimposed. Many different specimens were examined from each of the nine subfamilies shown in Fig. 1. The LL spectral response can be seen to be the dominating feature in all of the spectral examples in Fig. 6. (The spectra of Fig. 6 are from individual beetles chosen to be representative of the spectral shapes observed.) The dominant LL reflectance color was in the green wavelengths (500-560nm), but other wavelengths relating to the colors of red, blue and a broadband gold were observed. The *Ceratocanthus sp*. (Fig. 6(a)) showed a main LL peak corresponding to a red wavelength with oscillating peaks trailing into the near infra-red (NIR). The *Diabroctis mimas* (Fig. 6(b)) species has a broadband reflection (550-700nm), which produces a gold color on the front of the beetle's pronotum. The *Protaetia angustata pyrodera* (Fig. 6(c)) beetle's reflection is strong compared to the other specimens, which has two peaks, close together, which gives the beetle a red/green appearance. The next five beetles (*Gnorimus nobilis*, *Viridimicus aurescens*,

Phaenomeris besckei, *Augoderia nitidula* and *Melolontha melolontha*) (Fig. 6(d)-(h)) showed narrowband LL responses. The *Phaenomeris besckei* specimen (Fig. 6(f)) had this response was at a lower wavelength (460 nm) (blue). The *Melolontha melolontha* specimen (Fig. 6(h)) showed the weakest of all the CP responses with LR and RL responses being stronger than the LL, which was a single peak in the orange/red region. There is some spectral variation in shape with the *Cheirotonus battareli* (Fig. 6(i)) specimen having a tail feature at wavelengths higher than the peak. All the reflection spectra were taken from a fixed position at the top of the right elytra of the beetles, except the beetles *Diabroctis mimas, Augoderia nitidula, Melolontha melolontha* and *Cheirotonus battareli* (Fig. 6(b), (g)-(i)), where reflection from the pronotum were taken, as their elytra were not as significantly optically active.
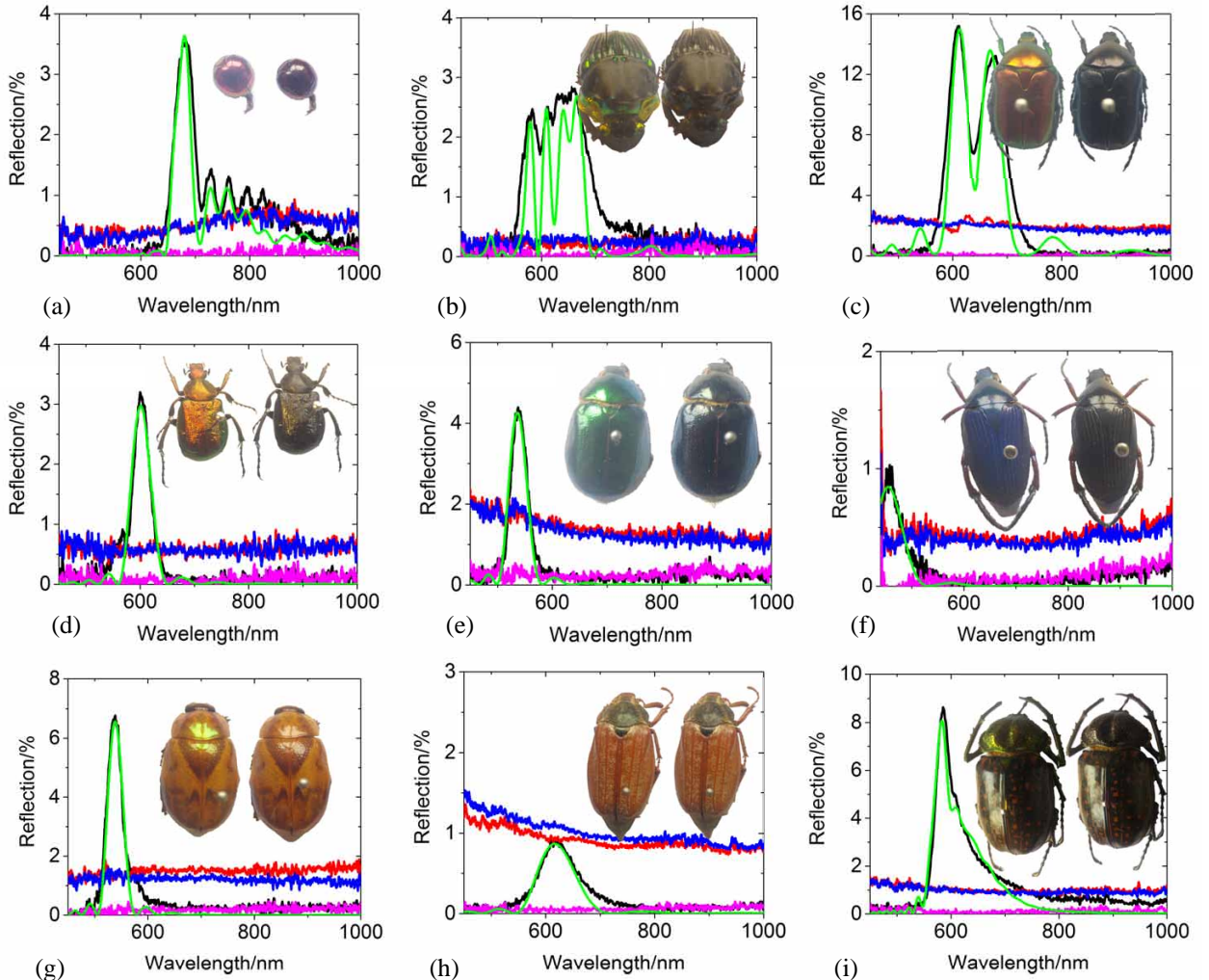

Fig. 6. CP reflection spectra with inset LCP (left) and RCP (right) filtered photographs of (a) Ceratocanthinae:*Ceratocanthus sp*. (b) Scarabaeinae:*Diabroctis mimas* (pronotum) (c) Cetoniinae:*Protaetia angustata pyrodera*. (d) Trichiinae:*Gnorimus nobilis*. (e) Rutelinae:*Viridimicus aurescens*. (f) Phaenomeridinae:*Phaenomeris besckei*. (g) Dynastinae:*Augoderia nitidula* (pronotum). (h) Melolonthinae:*Melolontha melolontha* (pronotum). (i) Euchirinae:*Cheirotonus battareli* (pronotum). Where experimental LL spectra are black, LR are red, RL are blue, RR are pink and modelled LL spectra are green.

Clear variation in the reflection percentage between beetles can be observed, there re several reasons for this including an increase in number or variation in the value of pitches within the beetle. Surface structure can inhibit the path of light to and from the helicoidal layer. [24]. The larger the curvature of the beetles' shells across the sample area means more light is scattered which is not collected by the detection optics and so the intensity is lower.

Chemical composition difference such as the addition of uric acid which enhances the birefringence and in turn increases the reflection [14] also contributes. The models in Fig. 6(d)-(h) were based on a single pitch, Fig. 6(a) and (i) were based on multiple pitches, Fig. 6(c) was with pitch defects and Fig. 6(b) was modelled with a combination of both. More in-depth studies were carried out on the Rutelinae and Cetoniinae subfamilies, which contain many variations in their CP responses. Variations to the single reflection spectral shape can be observed in species of *Cetoniinae:Cetonia aurata aurata* (which were distinguished from Protaetia cuprea by their prosternum [25]) beetles from Poland and Romania (Fig. 7). Previous studies have looked at the CP reflection from *C. aurata aurata* [26][27] using ellipsometric techniques from which the LL response can be determined. This current study looked at a much larger sample set and the experimental arrangement determined the LL response directly. In particular this study looked at the shapes of the spectra and their relation to the structure. Five spectral classifications were identified by the authors (although other classifications could be justified). Those chosen are single peaked (S), double close (DC), triple peaks (T), oscillations after (OA) and oscillations between peaks (X), whilst the remainder were grouped as unclassified (U). The models included in Fig. 7 are based on the same perturbation approach. Fig. 7(a) was based on a single pitch value, Fig. 7(b)-(d) pitch defects and Fig. 7(e) and (f) multiple pitch values.
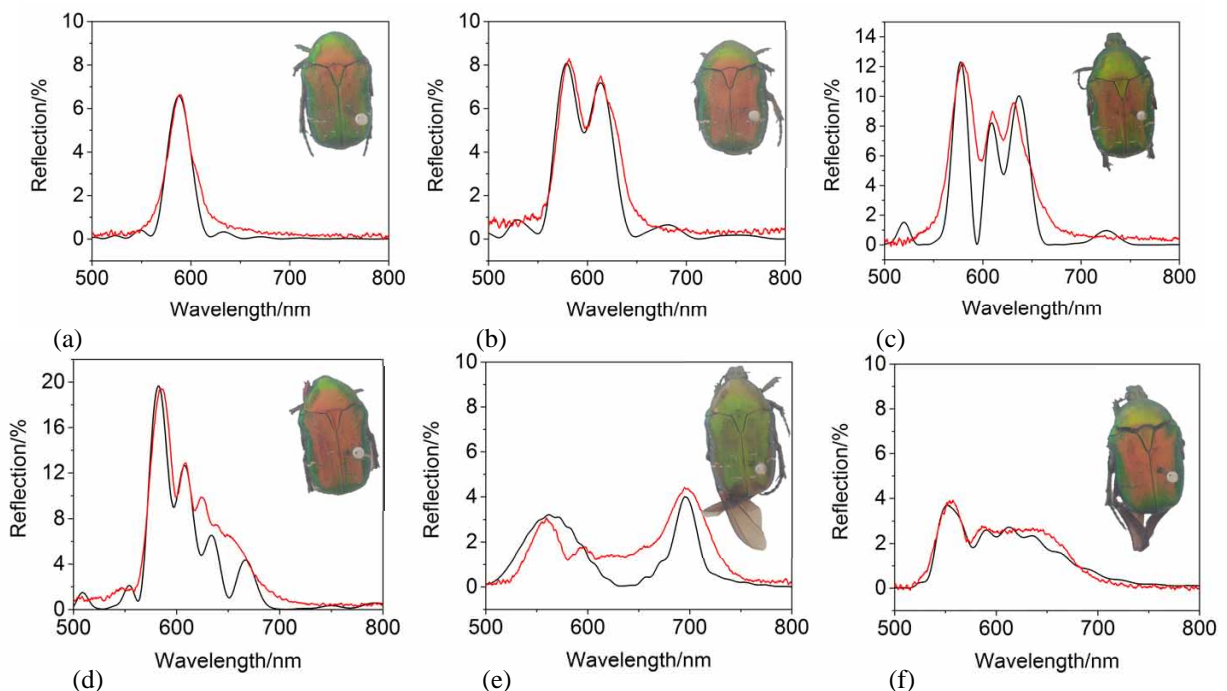

Fig. 7. LL spectral responses of *Cetonia aurata aurata* specimens with, described as (a) single peak (S), (b) double close (DC), (c) triple (T), (d) oscillations after (OA), (e) double apart (X) and (f) unclassified (U). The red lines are experimental data and the black are modelled. The inset photographs are of beetles through a LCP filter.

The distributions of LL spectral shapes of 191 *Cetonia aurata aurata* specimens (Fig. 8), shows that the single peak structure is not the dominating feature. The most common spectral shape was the OA feature, which occurred in 29.9% of the measured spectra, closely followed by DC (27.2%) and T (19.9%), while the single peak spectra only occurred in 13.1%.
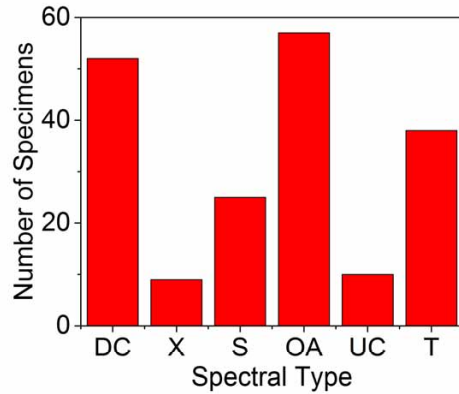
Fig. 8. Distribution of LL spectral shapes of *Cetonia aurata aurata s*pecimens.

The genus Rutelinae:*Chrysina* CP responses were very variable both between and within species (Fig. 9-10). The genus has a large geographic range from the Southern United States to Columbia. Fig. 9(a), shows the LL reflection from three distinct color forms (where silver is the most common color found) of *Chrysina optima* (it should be noted that there are more uncommon color forms such as violet [28]). The different color forms relate to the location of the lower wavelength reflection boundary. Where the red beetle's lower reflection boundary is 600nm, the gold boundary was 500nm and the silver boundary was lower than 450nm. Not only did spectral colors (wavelengths) change between species, the spectral intensity also varied. This was linked to the variation in thickness of the pitches within the structure, this was shown in the model (Fig. 9(b)) and based on the thicknesses and structure of the closely related *Chrysina aurigans* which has been modelled to include a chirped structure with slight perturbations to the regular structure [29].
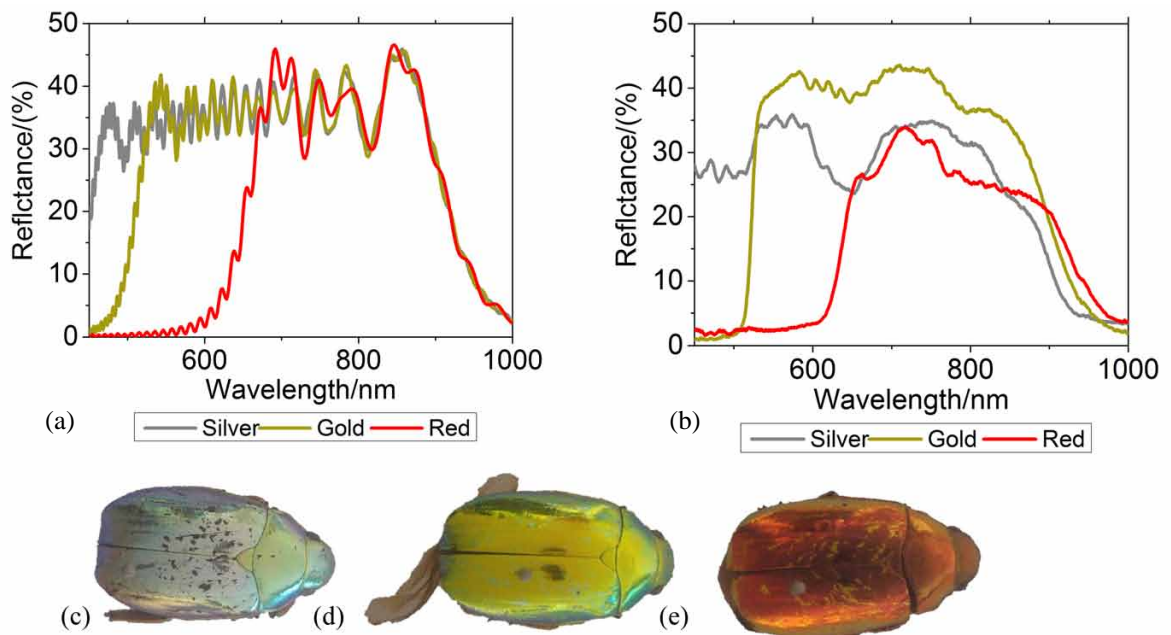

Fig. 9. *Chrysina optima* (a) experimental LCP spectral responses (b) modelled spectra responses, (c) photograph of the silver form through a LCP filter, (d) photograph of the gold form through a LCP filter and (e) photograph of the red form through a LCP filter.

The typical reflection spectrum of a silver *Chrysina chrysargyrea* (Fig. 10(a)), shows a strong LL response between 450nm and 900nm, with weak uniform LR and RL responses, and a negligible RR response. This LL spectrum with a long wavelength cut-off is distinct from the others modelled in this work and consideration of the structure giving rise to this is the subject of ongoing work. It should be noted that there are several other rare colour forms of *C chrysargyrea* including red and gold [28].
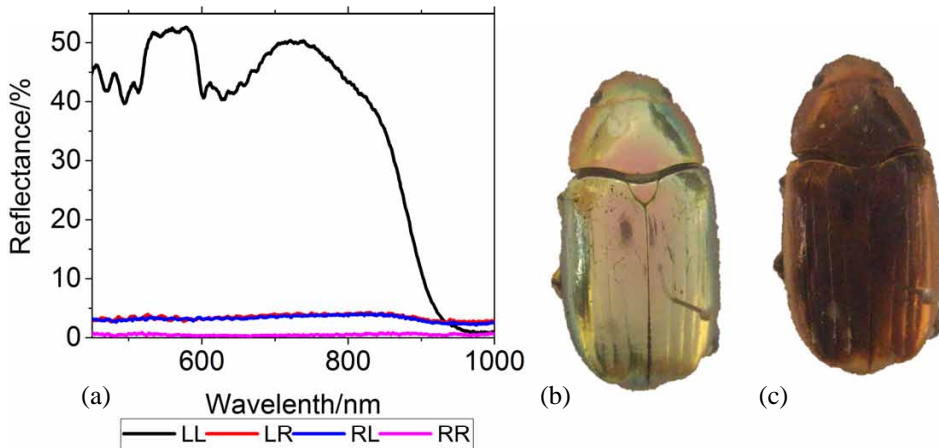

Fig. 10. *Chrysina chrysargyrea* silver form (a) CP spectral responses and photographs through (b) a LCP filter and (c) a RCP filter.

4. Discussion and Conclusion

The work presented shows variations within the helicoidal structures, responsible for the selective reflection of CP light, between and within some of the nine different subfamilies of Scarabaeoidae. Variations in spectral shape were observed in *Cetonia aurata aurata* specimens, which showed the single pitch structure is an atypical structure. The genus *Chrysina* was investigated and color differences of the broadband reflector *Chrysina optima*, were also observed. A model was developed to describe two possible perturbations of the helicoidal structure which would give rise to the observed spectra. These were based on a sudden change in the orientation of the chitin molecules, variation in the pitches and multiple pitches. Modelling comparison to the experimental results were made with good agreement. It should be noted that the reasons for the different reflection spectra within species is not fully understood and could be a combination of genetic [30] and environmental factors [31].

Acknowledgements

Appendix

Modelling parameters within this paper are described within this appendix.

Figure	Principal indices, $\bar{n} \pm \delta n$	$(N_1, p_1[\text{nm}]), \varphi_1, \dots \varphi_{m-1}, (N_m \cdot p_m[\text{nm}])$
6(a)	$1.51 + 0.006i \pm 2.6 \times 10^{-3}$	$(1, 673), 1, (1, 557), 1, (0.5, 536), 1, (0.5, 516), 1, (1.5, 496), 1, (2, 476), 1, (10, 445)$
6(b)	$1.513 + 0.005i \pm 7.5 \times 10^{-3}$	$(3.25, 207), 0.6, (3.25, 207), 0.75, (3.25, 207), 0.24, (3.25, 207)]$
6(c)	$1.488 + 0.0325i \pm 2.3 \times 10^{-3}$	$(4.0, 215), 0.5, (4, 207)$
6(d)	$1.493 + 0.005i \pm 0.75 \times 10^{-3}$	$(6.5, 202)$
6(e)	$1.49 + 0.008i \pm 1.0 \times 10^{-3}$	$(6.5, 180)$
6(f)	$1.49 + 0.008i \pm 7.5 \times 10^{-3}$	$(3.5, 306)$

6(g)	$1.49 + 0.005i \pm 10.0 \times 10^{-3}$	$(7.5, 362)$
6(h)	$1.49 + 0.008i \pm 7.5 \times 10^{-3}$	$(3.5, 415)$
6(i)	$1.50 + .017i \pm 20.0 \times 10^{-3}$	$(0.5, 454),1,(0.5,444),1,(0.5,433),1,(0.4,423),1,(0.4,412),1,$ $(0.4,402),1,(0.4,392),1,(10,382),1,(0.5,372),1,(0.5,362),1,(0.5,351),1,(0.5$ $\cdot 341),1,(0.5,331),1,(0.5,321),1,(0.5,310),1,(0.5,300)$
7(a)	$1.489 + .008i \pm 11 \times 10^{-3}$	$(7.5,395)$
7(b)	$1.489 + .025i \pm 22 \times 10^{-3}$	$(6,399),0.48,(5,399)$
7(c)	$1.506 + .025i \pm 10 \times 10^{-3}$	$(4.5,402),0.6,(4.5,402),0.33,(4.5,402)$
7(d)	$1.500 + .010i \pm 20 \times 10^{-3}$	$(3.5,403),0.067, (3.5,403),0.425, (3.5,403),0.425, (3.5,403)$
7(e)	$1.505 + .010i \pm 15 \times 10^{-3}$	$(4,372),1,(12,465),1,(3,398),1,(3,465),0,(3.5,465)$
7(f)	$1.506 + .018i \pm 16.5 \times 10^{-3}$	$(1.5,440),0,(1.5,406),1,(12,368)$

Each model structure consists of m stacks, $[\bar{n} \pm \delta n, (N_1, p_1), \varphi_1, \ldots \varphi_{m-1}, (N_m, p_m)]$ where $\bar{n} \pm \delta n$ are the transverse principal indices, N_i is the number of turns of pitch p_i(nm) for the ith stack, and φ_i is the twist discontinuity (in units of π) between stacks i and $i+1$.

References

[1]   A. Michelson, Philos. Mag., 21 (1911), 618–623
[2]   S. Vignolini, P. J. Rudall, a. V. Rowland, A. Reed, E. Moyroud, R. B. Faden, J. J. Baumberg, B. J. Glover, and U. Steiner, Proc. Natl. Acad. Sci. 109 (2012) 15712–15715
[3]   P. P. Shibayew and R. G. Pergolizzi, Int. J. Bot., 7 (2011) 113–117
[4]   J. Marshall, T. W. Cronin, N. Shashar, and M. Land, Curr. Biol. 9 (1999) 755–8
[5]   T. H. Chiou, S. Kleinlogel, T. Cronin, R. Caldwell, B. Loeffler, A. Siddiqi, A. Goldizen, and J. Marshall, Curr. Biol. 18 (2008) 429–434
[6]   Y. Baar, J. Rosen, and N. Shashar, PLoS One, 9 (2014). e86131
[7]   H. Wynberg, E. W. E. Meijer, J. C. Hummelen, H. P. J. M. Dekkers, P. H. Schippers, and A. D. Carlson, Nature 286 (1980) 641–642
[8]   T. W. Cronin and J. Marshall, Philos. Trans. R. Soc. Lond. B. Biol. Sci. 366 (2011) 619–626
[9]   J. Bailey, in Origins of Life and Evolution of the Biosphere, 2001, vol. 31, no. 1–2, pp. 167–183.
[10]   T. Lenau and M. Barfoed, Adv. Eng. Mater. 10 (2008) 299–314
[11]   J. D. Pye, Biol. J. Linn. Soc. 100 (2010) 585–596
[12]   M. E. McNamara, D. E. G. Briggs, P. J. Orr, H. Noh, and H. Cao, Proc. R. Soc. B Biol. Sci. 279 (2012) 1114–1121
[13]   A. C. Neville and S. Caveney, Biol. Rev. Camb. Philos. Soc. 44 (1969) 531–562
[14]   S. Caveney, Proc. R. Soc. B Biol. Sci. 178 (1971) 205–225
[15]   D. E. Azofeifa, H. J. Arguedas, and W. E. Vargas, Opt. Mater. (Amst) 35 (2012) 175–183
[16]   S. A. Jewell, P. Vukusic, and N. W. Roberts, New J. Phys. 9 (2007) 99–99
[17]   S. Y. Ching, G. Li, H. L. Tam, D. T. P. Goh, J. K. L. Goh, and K. W. Cheah, Opt. Mater. Express 4 (2014) 2340
[18]   Google, "Google Maps." [Online]. Available: https://www.google.com/maps/d/. [Accessed: 12-Jun-2016].
[19]   Ocean Optics, "DH-2000 BAL." [Online]. Available: http://oceanoptics.com/product/dh-2000-bal/. [Accessed: 20-Apr-2016].
[20]   E. Hecht, Optics, Addison-Wessley. 2001.
[21]   I. E. Carter, K. Weir, M. W. McCall, and A. R. Parker, R. Soc. Interface, 13 (2016) 20160015
[22]   M. W. McCall, I. J. Hodgkinson, and Q. H. Wu, Birefringent Thin Films and Polarizing Elements, 2nd ed. London: Imperial College Press, 2014.
[23]   V. I. Kopp and A. Z. Genack, Phys. Rev. Lett. 89 (2002) 033901
[24]   M. Xu, A. E. Seago, T. D. Sutherland, and S. Weisman, J. Morphol. 271 (2010) 1300–5
[25]   P. Zagatti and A. Guy, 2005. [Online]. Available: http://www.insecte.org/photos/archives/Cle_Cetoines_de_France_P_Zagatti.pdf. [Accessed: 03-Jun-2015].
[26]   H. Arwin, T. Berlind, B. Johs, and K. Järrendahl, Opt. Express 21 (2013). 22645–22656
[27]   X. Wu, Structure-property-relations of Cuticular Photonic Crystals Evolved by Different Beetle Groups (Insecta, Coleoptera). Berlin: epubli GmbH, 2014.
[28]   A. Solís, [online] available http://www.inbio.ac.cr/papers/Plusiotis/Chrysina.html [accessed 05-Aug-2016]
[29]   D. E. Azofeifa, M. Hernández-Jiménez, E. Libby, a. Solís, C. Barboza-Aguilar, and W. E. Vargas, J. Quant. Spectrosc. Radiat. Transf. 160 (2015). 63–74
[30]   S. Velez and J. L. Feder, Mol. Ecol. 15 (2006) 1393–1404
[31]   K. Yamamoto, Y. Tsujimura, M. Kometani, C. Kitazawa, A. T. M. F. Islam, and A. Yamanaka, J. Insect Physiol. 57 (2011). 930–4